CHEST IMAGING
Iran J Radiol. 2023 January; 20(1):e130478. https://doi.org/10.5812/iranjradiol-130478.
Published online 2023 March 6. **Research Article**

Cystic and Cavitary Lung Cancer: Its Characteristic Features on CT and FDG-PET Scans

Makiko Murota [1,*], Takashi Norikane [1], Yuka Yamamoto [1], Mariko Ishimura [1], Katsuya Mitamura [1], Yasukage Takami [1], Kengo Fujimoto [1], Katashi Satoh [2], Naoya Yokota [3], Ryou Ishikawa [4] and Yoshihiro Nishiyama [1]

[1]Department of Radiology, Faculty of Medicine, Kagawa University, Miki-cho, Japan
[2]Department of Radiology, Diagnostic Imaging Center, Utazu Hospital, Utazu-cho, Japan
[3]Department of General Thoracic Surgery, Faculty of Medicine, Kagawa University, Miki-cho, Japan
[4]Department of Diagnostic Pathology, Faculty of Medicine, Kagawa University, Miki-cho, Japan

[*]*Corresponding author*: Department of Radiology, Faculty of Medicine, Kagawa University, Miki-cho, Japan. Email: murota.makiko.kc@kagawa-u.ac.jp

Received 2022 August 15; **Revised** 2023 January 17; **Accepted** 2023 January 23.

Abstract

Background: Cystic and cavitary lung cancer (CCLC) is infrequently observed on computed tomography (CT) scans; however, its diagnosis is often overlooked or delayed.
Objectives: The current study aimed to investigate the CT and ^{18}F-fluorodeoxyglucose positron emission tomography (^{18}F-FDG PET) features of CCLC.
Patients and Methods: A total of 809 patients who underwent lung tumor resection were examined in this study, and the presence of cystic and cavitary lesions on CT scans was investigated. Based on the CT scans, CCLC was identified in 102 consecutive patients. The diameters of the whole nodule and the airspace portion of the lesion, morphological patterns of cystic and cavitary lesions, presence of ground glass opacity (GGO), and loculation pattern (including the presence of a septum) were evaluated. The positron emission tomography (PET) scans of CCLC were also assessed visually and semi-quantitatively.
Results: A total of 104 CCLC lesions were evaluated in this study. The histological analysis indicated 85 cases of adenocarcinoma (AD) and 19 cases of squamous cell carcinoma (SCC). The morphological patterns of cystic and cavitary lesions were classified into four types. The presence of GGO, type 4 morphological pattern (a soft-tissue-density structure intermixed within clusters of a cavitary lesion), and multilocular with septum (MS) loculation pattern were significantly different according to the histological type. The maximum standardized uptake value (SUV_{max}) on PET scans was significantly lower in AD compared to SCC ($P = 0.002$). In the solid nodule part of cystic and cavitary lesions, the MS pattern was significantly more common in AD ($P = 0.044$).
Conclusion: When cystic and cavitary lesions are observed on CT scans, the presence of GGO and the MS pattern should be considered, as it may help differentiate the histological findings.

Keywords: Thin-walled Cavity, Cystic, Lung Cancer, Computed Tomography, Positron Emission Tomography

1. Background

Lung cancer is the most common cause of cancer mortality worldwide, accounting for 18.4% of all cancer-related deaths (1). According to the National Lung Screening Trial (NLST), application of low-dose computed tomography (CT) for annual screening caused a relative reduction of 20% in lung cancer mortality over three years compared to chest X-ray (2). The Nederlands-Leuvens Longkanker Screenings Onderzoek (NELSON) study also reported a significant difference in the reduction of lung cancer mortality with low-dose CT screening (3). On the other hand, several studies have shown that lung cancer may appear as thin-walled cavitary or cystic lesions on CT scans (4-7). These lesions are referred to as "lung cancer associated with cystic airspaces," "thin-walled cavity lung cancer," "cystic lung cancer," and so on; however, the nomenclature for these lesions is not well established (8). In the present study, these lesions are referred to as "primary cystic and cavitary lung cancer (CCLC)."

The diagnosis of CCLC may be missed or delayed in some cases; for example, in the NELSON trial, bulla wall thickening was observed in 22% of missed lung cancer cases on CT scans (8, 9). The Fleischner Society guidelines for the management of incidental nodules on CT scans suggest that management of CCLC is strongly influenced by the appearance of the nodule, such as wall thickening of

the cystic lesion and its size (10). In high-risk individuals, CT screening for lung cancer focuses on early detection; however, there are no detailed CT findings in patients with CCLC. Currently, there are no recommendations or clinical guidelines for the surveillance of CCLC in routine practice or screening (11). Few studies on CCLC have investigated the findings of ^{18}F-fluorodeoxyglucose positron emission tomography (^{18}F-FDG PET); however, even when findings are available, the number of patients is relatively small (4, 5). Similarly, the relationship between the CT findings of patients with CCLC and ^{18}F-FDG accumulation on PET images has not been investigated.

2. Objectives

The present study aimed to thoroughly describe the CT and ^{18}F-FDG PET findings of patients with CCLC.

3. Patients and Methods

3.1. Patients

The Ethics Committee of our institution approved this retrospective study, and the requirement to obtain consent was waived (No.: 2020-711). The medical records of patients presenting to our hospital were reviewed. A total of 809 patients, who underwent pulmonary resection for primary lung cancer, were examined from March 2013 to September 2019, and the presence of cystic and cavitary lesions on CT scans was investigated.

3.2. CT Scans

CT scans were obtained using a 64-slice multidetector row CT (MDCT) scanner (Aquilion 64, Canon Medical Systems, Japan) and a 256-slice MDCT scanner (Brilliance iCT, Philips Healthcare, USA). An X-ray tube voltage of 120 kV and a current of 300 mA were used in all examinations. All patients were scanned in the supine position upon full inspiration.

3.3. 18F-FDG-PET/CT Imaging

The ^{18}F-FDG PET scans were acquired using a PET/CT scanner (Biograph mCT, SIEMENS, Germany). The patients were asked to fast for at least five hours before the ^{18}F-FDG PET examinations. All the participants received 5 MBq of ^{18}F-FDG per kilogram of body weight. The mean interval between ^{18}F-FDG injection and scanning was 90 minutes.

3.4. Image Analysis

All CT scans were reviewed at a window width of 1600 HU and a window level of -700 HU on an EV Insite viewer (PSP Corp., Japan). First, a thoracic radiologist (with 10 years of experience) searched for lung cancer and flagged cystic and cavitary lesions on CT scans, except for obvious necrotic cavities with low-density areas and fluid retention, suggesting a necrotic material inside, bronchiectasis, and a preexisting bulla (Figure 1). Next, two thoracic radiologists (with six and 21 years of experience, respectively) reviewed the flagged images independently and resolved any discrepancies by reaching a consensus. To prevent any potential bias, the clinicopathological characteristics of the patients were not known in advance. The radiologists evaluated the CT findings, including the presence of emphysema, bulla, and interstitial pneumonia.

The anatomical distribution was classified according to the lobe of the lung. It was considered predominantly peripheral if the lesion was limited to the outer one-third of the lung. The diameters of the whole nodule and the airspace portion of the lesion were calculated in this study. The morphological patterns of cystic and cavitary lesions were classified into four types: Type 1, a nodule extruding the wall of the cavitary lesion; type 2, a nodule within the cavitary lesion; type 3, thickening of the wall and/or soft tissue density around the cavitary lesion; and type 4, a soft-tissue-density structure intermixed within clusters of a cavitary lesion (Figure 2) (4, 5, 12).

Additionally, the presence of ground glass opacity (GGO) and the loculation pattern (e.g., presence of septum) were evaluated in this study. By reviewing all CT scans and referring to a previous study (4), the loculation pattern was classified into four types: (1) unilocular; (2) multilocular; (3) unilocular with a septum; and (4) multilocular with a septum (MS) (Figure 3). The ^{18}F-FDG PET scans, if available, were visually and semi-quantitatively assessed by the two radiologists (mentioned above), who had sufficient experience in the interpretation of ^{18}F-FDG PET scans.

The visual assessment was finally rated on a three-point scale (absent, moderate, and marked) (4). The uptake was considered "absent" when it was isointense to the lung, "moderate" when it was isointense relative to the mediastinal blood pool, and "marked" when it was hyperintense relative to the mediastinal blood pool. One of the radiologists performed a semi-quantitative assessment, based on the standardized uptake value (SUV). The maximum SUV (SUV_{max}) was defined as the highest SUV value on a pixel within the region of interest.

3.5. Statistical Analysis

Statistical analyses were performed in SPSS version 24 (IBM Corp. Released 2016. IBM SPSS Statistics for Windows,

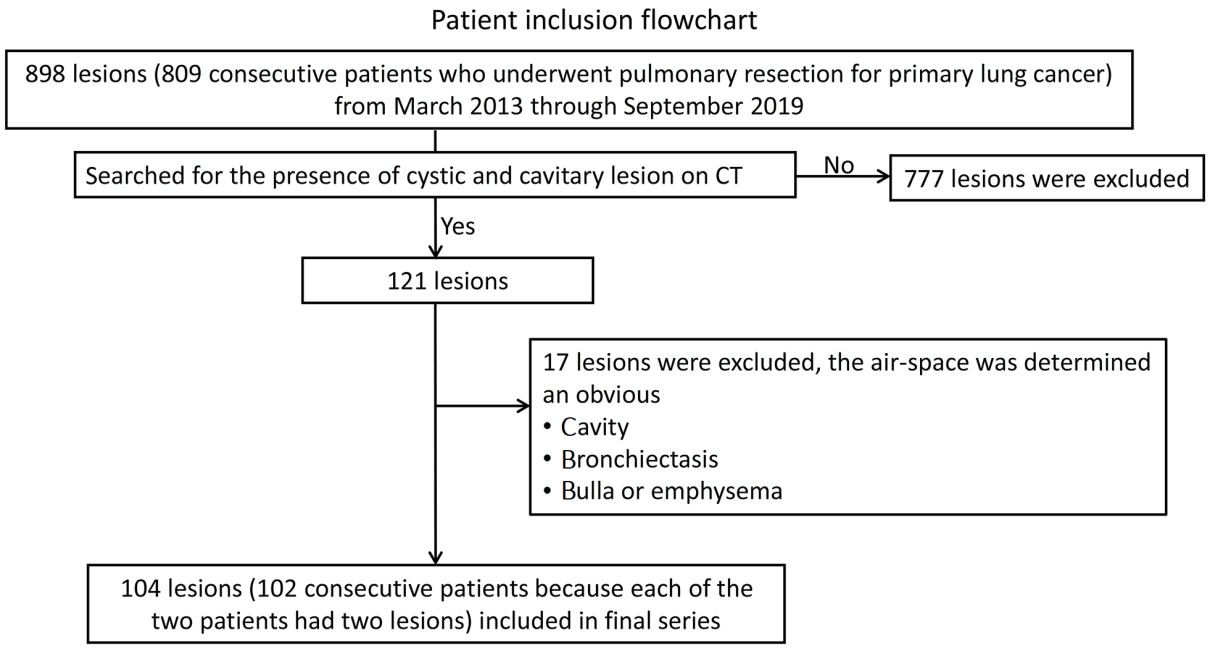

Figure 1. The flowchart of patient enrollment

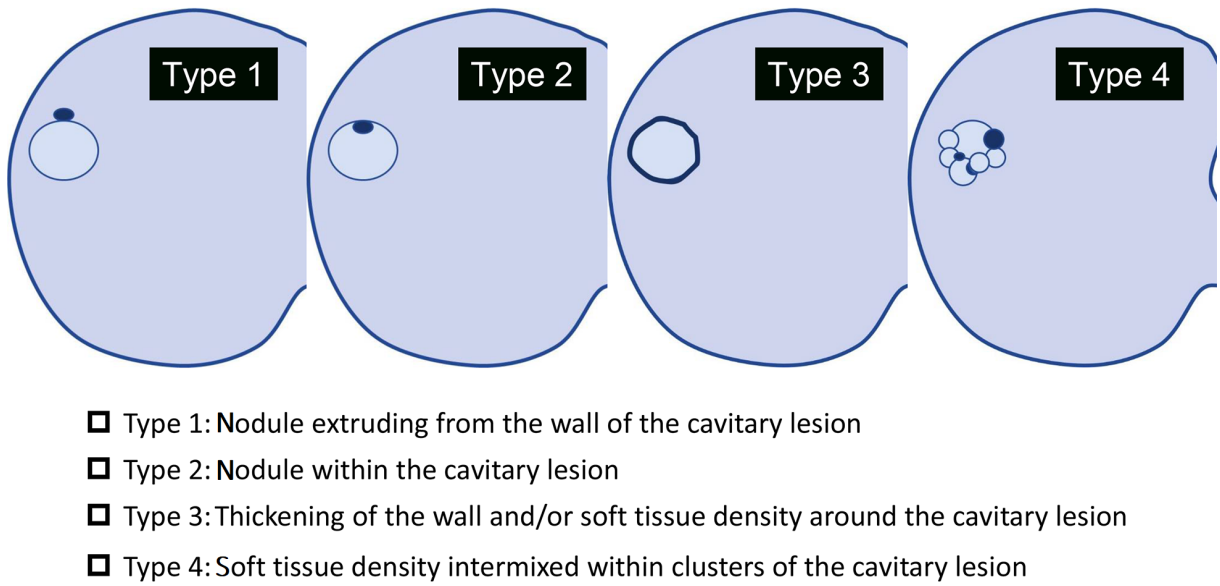

Figure 2. Morphological patterns of cystic and cavitary lesions. The image shows the morphological patterns of cystic and cavitary lung cancer (CCLC), classified into four types as proposed by Mascalchi et al. (5) (type 1, nodule extruding the wall of cavitary lesion; type 2, nodule within the cavitary lesion; type 3, thickening of the wall and/or soft tissue density around the cavitary lesion; and type 4, a soft-tissue-density structure intermixed within clusters of cavitary lesion).

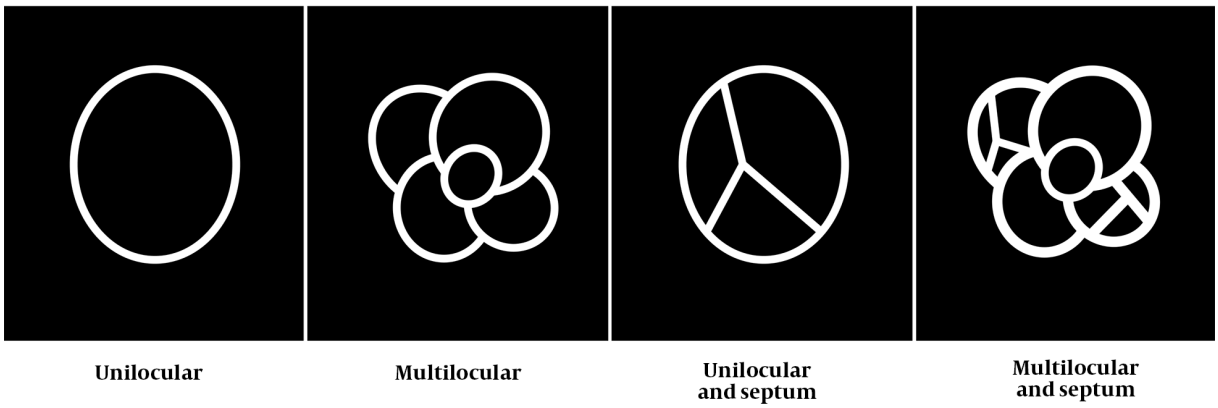

Figure 3. Loculation patterns, including the presence of septum. The loculation patterns for cystic and cavitary lung cancer (CCLC) are classified into four types according to a study by Fintelmann et al. (4), while considering the presence of septum: Unilocular; multilocular; unilocular with a septum; and multilocular with a septum (MS).

Version 24.0. Armonk, NY: IBM Corp.). Continuous variables with a normal distribution are presented as mean ± standard deviation (SD), and variables without a normal distribution are reported as median with the 25th and 75th interquartile ranges (IQR). Categorical variables are presented as number and percentage. Chi-square (χ^2) test and Fisher's exact test were used to analyze categorical variables. Kolmogorov-Smirnov test was also performed to determine whether the data were normally distributed. Mann-Whitney U test was used for data without a normal distribution. Moreover, age, data pertaining to the lesion diameter on CT scans, SUV_{max}, and visual assessment results based on FDG-PET/CT scans were compared using Mann-Whitney test. The level of statistical significance was set at $P \leq 0.05$ for all tests.

Inter-observer agreement regarding the presence or absence of CT findings was analyzed by calculating Cohen's kappa coefficient (12) in assessments performed before reaching a consensus with the thoracic radiologist who reviewed the images. The inter-observer agreement was classified as follows: Excellent ($\kappa = 0.81$ - 1.00), substantial ($\kappa = 0.61$ - 0.80), moderate ($\kappa = 0.41$ - 0.60), fair ($\kappa = 0.21$ - 0.40), and poor ($\kappa = 0$ - 0.20).

4. Results

4.1. Description of CT Findings

A total of 102 consecutive patients (79 men and 23 women; mean age, 69.7 ± 1.0 years; age range, 22 - 91 years) with CCLC on CT scans were included in this study. There were 898 resected lesions of primary lung cancer. Since two patients had two lesions each, 11.6% of lesions (104/898 lesions) showed CCLC on CT scans. The histological analysis indicated adenocarcinoma (AD) in 85 out of 104 lesions (81.7%) and squamous cell carcinoma (SCC) in 19 (18.3%) lesions. The AD spectrum lesions included invasive AD in 66 (63.4%) lesions, AD in situ in 6 (5.8%) lesions, and minimally invasive AD in 13 (12.5%) lesions (Figures 4 and 5).

Based on the results, CCLC was identified in the right upper lobe, right middle lobe, right lower lobe, left upper lobe, and left lower lobe in 25 (24.1%), 10 (9.6%), 31 (29.8%), 15 (14.4%), and 23 (22.1%) lesions, respectively. Also, CCLC was identified in the peripheral in 81 (79.3%) lesions. There was no significant difference in the cancer location between AD and SCC. Regarding the background lung parenchyma, 52 patients showed pulmonary emphysema, and 22 patients had pulmonary fibrosis. The average tumor size of CCLC was 3.0 ± 1.9 cm (range, 0.6 - 11.4 cm), and the average airspace diameter was 1.9 ± 1.7 cm (range, 0.2 - 10.5 cm). The CT findings are presented in Table 1, and the CT findings based on the histopathological subtype are presented in Table 2.

According to the findings, GGO was present in 62 out of 104 lesions, including 60 (96.8%) AD and two (3.2%) SCC lesions. The most common morphological pattern of CCLC was type 4 in 38 (36.6%) lesions, followed by type 3 in 36 (34.5%) lesions. Regarding the presence of GGO by the morphological pattern, 12/29 (41.4%), 0/1 (0.0%), 16/36 (44.4%), and 34/38 (89.5%) lesions were classified as type 1, 2, 3, and 4, respectively. Considering the loculation pattern (Figure 3), the MS pattern was the most common pattern, detected in 59 (56.8%) lesions. Regarding the presence of GGO by the loculation pattern, 5/10 (50.0%), 5/7 (71.4%), 14/28 (50.0%), and 38/59 (64.4%) lesions showed unilocular, multilocular, unilocular with a septum, and MS patterns, respectively. The presence of GGO was significantly more common in AD than SCC ($P < 0.001$).

The frequencies of the morphological pattern type 4 (P

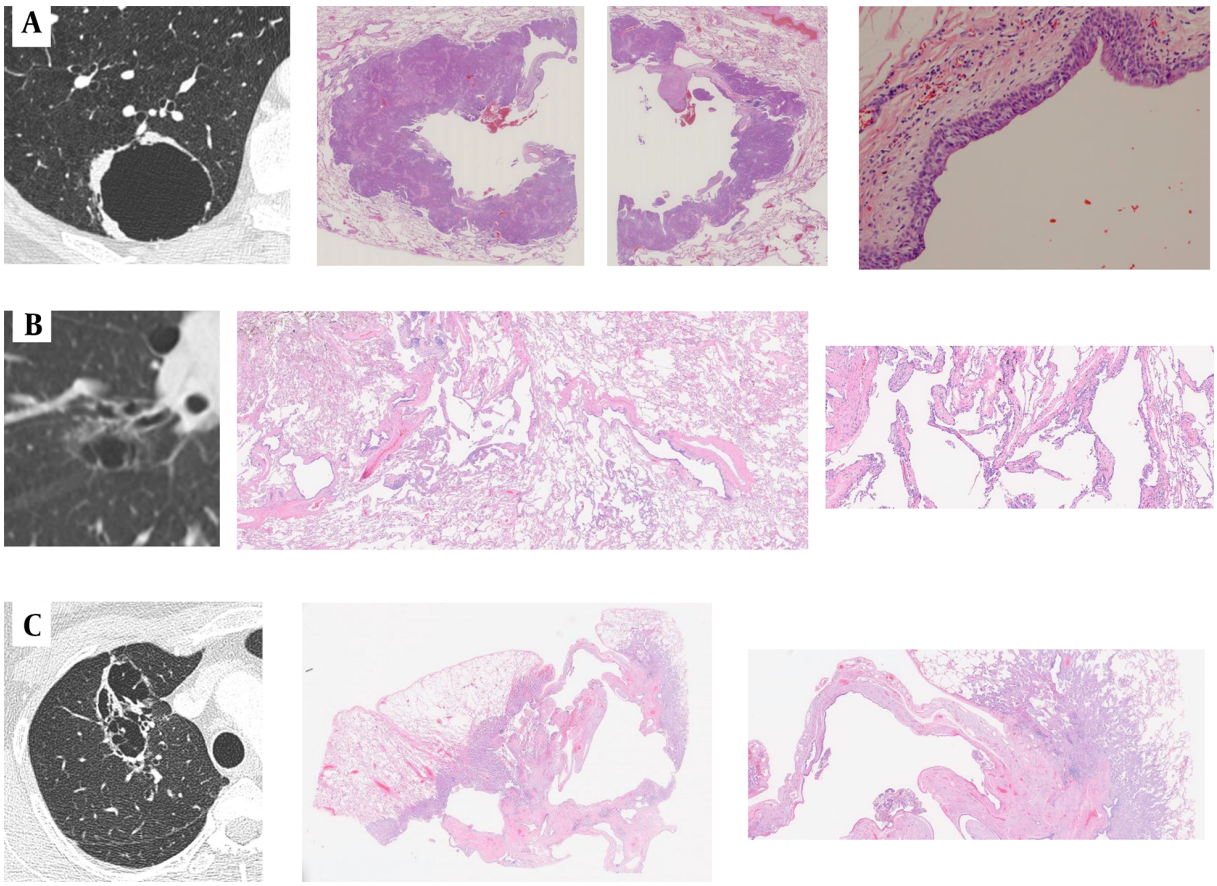

Figure 4. A, A 66-year-old man with cystic and cavitary lung cancer (CCLC). The CT scan shows a type 3, unilocular pattern with irregular wall thickening. A histopathological diagnosis of squamous cell carcinoma (SCC) is made. The low-power histological image shows a cystic airspace without septa; B, A 75-year-old man with CCLC. The CT scan shows a type 1, unilocular with septum pattern with subtle ground glass opacity (GGO). A histopathological diagnosis of adenocarcinoma (AD) in situ is made. The low-power histological image shows a cystic airspace with a septum, the alveolar walls of which are more fibrously thickened than those of typical AD in situ; C, A 52-year-old woman with CCLC. The CT scan shows a type 4, multilocular with septum pattern with subtle GGO. A histopathological diagnosis of invasive AD is made. The low-power histological image shows a cystic airspace with a multilocular pattern and septa, which are dilated bronchi and blood vessels. The histopathological findings suggest that the bronchi may be dilated against a relatively large bronchus packed by the tumor, and the bronchovascular bundle in the cavity-like area may be dilated with fibrous thickening, showing a septum-like structure.

= 0.016) and the MS pattern ($P < 0.05$) were significantly higher in AD than SCC (Table 2). The inter-observer agreement for identifying the presence of GGO was excellent (κ = 0.86). Also, the inter-observer agreement was moderate and substantial for the identification of the morphological pattern and loculation pattern of CCLC (κ = 0.58 and κ = 0.64, respectively).

4.2. Description of 18F-FDG-PET/CT Findings

The ^{18}F-FDG-PET/CT scans were available for 66 (63.5%) lesions. The visual assessment indicated absent uptake in 2 (3.0%) out of 66 lesions, moderate uptake in 8 (12.1%) lesions, and marked uptake in 56 (84.9%) lesions (Figure 5). The inter-observer agreement for the visual assessment was excellent (κ = 0.91). There were no significant differences in the overall visual assessment or in the evaluation of only solid lesions. The average SUV_{max} of CCLC was 6.5 ± 4.9. The SUV_{max} was significantly lower in AD than SCC on PET scans (P = 0.002).

4.3. Description of CT and 18F-FDG PET/CT Findings of Solid Lesions

There was no significant difference in the average SUV_{max} when only CCLC lesions with a solid component without GGO were assessed. Among solid lesions, only the MS pattern on CT scans was significantly more common in AD than SCC (P = 0.044).

5. Discussion

The CT scans of 104 lesions and ^{18}F-FDG-PET/CT scans of 66 lesions with CCLC were evaluated in the present study.

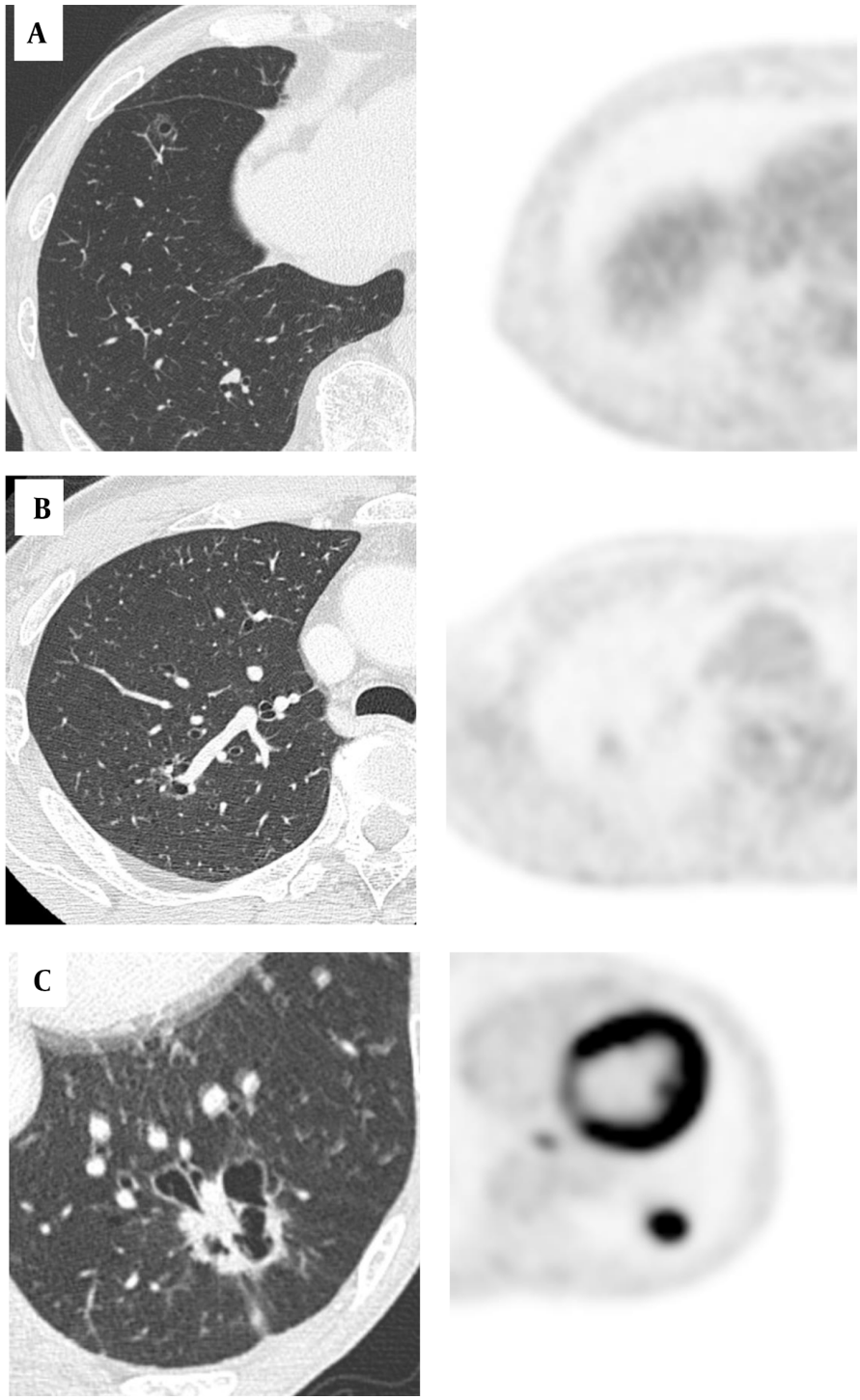

Figure 5. The CT scans and corresponding fluorodeoxyglucose positron emission tomography (FDG-PET) images of cystic and cavitary lung cancer (CCLC). Top row: A, An 80-year-old man with minimally invasive adenocarcinoma (AD); the FDG-PET scan shows absent uptake (maximum standardized uptake value [SUV_{max}] = 0). Middle row: B, A 60-year-old man with invasive AD; the FDG-PET scan shows moderate uptake (SUV_{max} = 1.24). Bottom row: C, A 68-year-old woman with squamous cell carcinoma (SCC); the FDG-PET scan shows marked uptake (SUV_{max} = 8.61).

Table 1. The Computed Tomography Findings of Cystic and Cavitary Lung Cancer

CT findings	No. (%) (total = 104)	κ
Consistency		0.75
Solid	42 (40.4)	0.86
Non-solid	8 (7.7)	0.53
Partly solid	54 (51.9)	0.73
GGO	62 (59.6)	0.86
Morphological patterns of CCLC		0.58
Type 1 [a]	29 (27.9)	0.63
Type 2 [b]	1 (1.0)	N.A.
Type 3 [c]	36 (34.5)	0.54
Type 4 [d]	38 (36.6)	0.59
Loculation pattern		0.64
Unilocular pattern	10 (9.6)	0.67
Multilocular pattern	7 (6.7)	0.56
Unilocular with a septum pattern	28 (26.9)	0.54
MS pattern	59 (56.8)	0.74

Abbreviations: CT, computed tomography; CCLC, cystic and cavitary lung cancer; GGO, ground glass opacity; κ, kappa coefficient (inter-observer); N.A., not applicable; MS, multilocular with a septum pattern.
[a] Nodule extruding the wall of cavitary lesion
[b] Nodule within the cavitary lesion
[c] Thickening of the wall and/or soft tissue density around the cavitary lesion
[d] A soft-tissue-density structure intermixed within clusters of the cavitary lesion

The incidence of CCLC based on the reviewed CT scans was 11.6% of all resected lung lesions. In a lung cancer screening setting, Farooqi et al. found that 3.7% of lung cancers presented with a cystic airspace (13, 14). Moreover, the incidence of CCLC was estimated at 0.46% in a surgical series (15). However, Byrne et al. recently reported an incidence rate of 9.3% in a surgical series (11). In the present study, the incidence of CCLC was higher than previous reports. Most patients with CCLC had AD (81.7%), followed by SCC (18.3%), as similarly indicated in previous research (88.1% and 9.1%, respectively) (16). Similar to previous reports, GGO on CT scans was a characteristic finding of cavitary AD lesions (17).

Currently, the guidelines for the management of pulmonary nodules, found incidentally or via lung cancer screening CT, do not specifically include lung cancer associated with cystic airspaces (16). Mendoza et al. suggested that when these cystic lesions are identified in high-risk individuals as part of lung cancer screening, decision-making about follow-up imaging or interventions based on the solid or GGO component rather than the cyst may be more suitable (16). Besides, they recommended that it may be safe to monitor a simple thin-walled cyst without a solid or GGO component as part of routine lung cancer screening annually.

The CT features of the morphological pattern were divided into four types, as described in previous research (4, 5, 13). In this study, type 4 (36.5%) and type 3 (34.5%) patterns were almost as frequent as each other, which is in line with the findings of a study by Mascalchi et al. (5). The type 4 pattern was significantly more common in AD than SCC, perhaps due to the higher frequency of GGO in type 4 (89.5%). In a previous report, the loculation pattern was only considered to be unilocular or multilocular (4). Regarding the loculation pattern, we also considered the presence of septum, as several previous studies showed that the presence of septum within CCLC is important (6, 7, 18-22). The presence of septum in CCLC was reported in 54.8 - 66.7% of cases (7, 18-21).

Liu et al. reported "separations within cavities" (44.4%) and "blood vessels passing through cavities" (20.2%) separately on CT scans (22). However, since it is often difficult to distinguish between these two types, many studies have not differentiated them (6, 7, 18-21). In the current study, septum in CCLC was observed in 83.7% of cases, which is higher than previous reports. Tan et al. also reported that septations within CCLC on CT scans were composed of different types of tissue, that is, fibrous tissues produced by tumor cells, bronchus, or blood vessels (7). The present findings showed that the MS pattern was significantly more common in AD than SCC, suggesting the need to consider the loculation pattern, not only GGO in CCLC on CT scans.

Although the developmental mechanism of solitary CCLC is uncertain, some studies of radiology-pathology correlations revealed that it is commonly caused by a check-valve mechanism, obstructing the small airways (in 38% of cases) (13). Other causes include lepidic growth of AD on emphysematous pulmonary parenchyma, cyst formation of a tumor, and growth along the wall of a preexisting bulla. In a study by Tan et al., microscopic findings revealed that most tumor cells produced abundant fibrous tissues, which might extrinsically cause airway obstruction and allow air to enter, but not exit ("ball-valve phenomenon"), leading to the development of cysts (7). The persistence of blood vessels and bronchi as relatively robust tissues and the pathological characteristics of tumor cells producing abundant fibrous tissues may contribute to the formation of septa (7).

Frequently, SCC is more extensively destructive than AD. The MS pattern is significantly more common in AD than SCC, possibly because its relatively stronger tissues are more likely to remain (17). According to the present histopathological study, the following mechanisms underlie the formation of the MS pattern of thin-walled cavities: (1) dilatation of bronchi against a relatively large bronchus,

Table 2. Clinical Characteristics of Patients and Computed Tomography Findings According to the Histopathological Subtype of Cystic and Cavitary Lung Cancer [a]

Clinical characteristics of patients	Number of patients		P-value
	AD (n = 85)	SCC (n = 19)	
Sex			0.328
Male	65 (76.5)	16 (84.2)	
Female	20 (23.5)	3 (15.8)	
Age	69.0 (65.0 - 76.0)	70.0 (68.0 - 73.0)	0.347
CT findings			
Tumor size	24.8 (20.6 - 35.9)	23.9 (16.7 - 40.9)	0.873
Airspace size	12.7 (10.3 - 20.8)	12.7 (7.4 - 22.4)	0.696
GGO	60 (70.6)	2 (10.5)	< 0.001*
Morphological patterns of cystic and cavitary lesions			0.016 *
Type 1 [b]	21 (24.7)	8 (42.1)	
Type 2 [c]	1 (1.2)	0 (0.0)	
Type 3 [d]	26 (30.6)	10 (52.6)	
Type 4 [e]	37 (43.5)	1 (5.3)	
Loculation			< 0.05 *
Unilocular pattern	6 (7.1)	4 (21.1)	
Multilocular pattern	6 (7.1)	1 (5.3)	
Unilocular with a septum pattern	20 (23.4)	8 (42.1)	
MS pattern	53 (62.4)	6 (31.6)	

Abbreviations: CCLC, Cystic and cavitary lung cancer; AD, adenocarcinoma; SCC, squamous cell carcinoma; GGO, ground glass opacity; MS, multilocular with a septum pattern.
[a] Values are expressed as No. (%) or median (interquartile ranges).
[b] Nodule extruding the wall of the cavitary lesion
[c] Nodule within the cavitary lesion
[d] Thickening of the wall and/or soft tissue density around the cavitary lesion
[e] A soft-tissue-density structure intermixed within clusters of the cavitary lesion

compressed by the tumor, and dilatation of the cavity-like portion of the bronchovascular bundle with a septum-like structure and fibrous thickening; (2) fibrous thickening of the alveolar septum associated with the tumor; and (3) fibrous thickening of a subpleural interlobular septum.

On ^{18}F-FDG PET scans, the SUV_{max} of AD was significantly lower than that of SCC (P = 0.001). Thin-walled cystic lesions and small mural nodules of CCLC may not demonstrate ^{18}F-FDG uptake. Also, depending on the amount of lepidic growth in AD, observed as GGO on CT scans, uptake on ^{18}F-FDG PET may be reduced or even absent (13). The present results also showed no significant difference in either visual or semi-quantitative analyses when only solid lesions were assessed. However, CCLC in AD often shows an MS pattern in the airspace on CT scan, even if the lesion is solid; this finding may help differentiate the histological findings and indicate a suspicion of lung cancer.

This study had several limitations. First, there could be selection bias in this retrospective study. Second, the present study was only based on temporary CT scans, and the morphological changes of CT scans over time remain unknown; therefore, morphological changes and the timing of images were not examined. Third, the radiology-pathology correlation was not determined in all cases. However, by reviewing the CT and ^{18}F-FDG PET images of many patients, it was possible to identify the characteristics of CCLC. Finally, in this study, the CT and PET features of CCLC were not compared with those of other non-cavitary lung cancers or non-tumoral lesions with cavitary changes, and survival was not analyzed; these variables need to be examined in future studies.

In conclusion, the CT features of CCLC, especially the presence of GGO and the MS pattern were more common in AD than SCC. The MS pattern was common in solid AD lesions. The ^{18}F-FDG uptake in AD was significantly lower than SCC, although there was no significant difference among solid lesions. Overall, the presence of an MS pattern in cystic airspaces on CT scans should be considered, as it may help differentiate the histological findings and identify potential lung cancer cases.

Footnotes

Authors' Contributions: Study concept and design: M. M. and K. S.; analysis and interpretation of data: M. I., N. Y. and R. I.; drafting of the manuscript: M. M.; critical revision of the manuscript for important intellectual content: T. N., Y. Y., K. M., Y. T., K. F. and Y.N.; statistical analysis: M. M.

Conflict of Interests: The authors declare no conflict of interests.

Data Reproducibility: All datasets used in the current study are available from the corresponding author on reasonable request.

Ethical Approval: This study was approved under the ethical approval code, IC-2020-171.

Funding/Support: We did not receive any funding from any profit or not-for-profit organizations for the research, authorship, or publication of this article.

Informed Consent: The requirement to obtain informed consent was waived because of the retrospective design of the study.

References

1. Bray F, Ferlay J, Soerjomataram I, Siegel RL, Torre LA, Jemal A. Global cancer statistics 2018: GLOBOCAN estimates of incidence and mortality worldwide for 36 cancers in 185 countries. *CA Cancer J Clin*. 2018;**68**(6):394–424. [PubMed ID: 30207593]. https://doi.org/10.3322/caac.21492.
2. Aberle DR, Adams AM, Berg CD, Black WC, Clapp JD; National Lung Screening Trial Research Team, et al. Reduced lung-cancer mortality with low-dose computed tomographic screening. *N Engl J Med*. 2011;**365**(5):395–409. [PubMed ID: 21714641]. [PubMed Central ID: PMC4356534]. https://doi.org/10.1056/NEJMoa1102873.
3. Horeweg N, Scholten ET, de Jong PA, van der Aalst CM, Weenink C, Lammers JW, et al. Detection of lung cancer through low-dose CT screening (NELSON): a prespecified analysis of screening test performance and interval cancers. *Lancet Oncol*. 2014;**15**(12):1342–50. [PubMed ID: 25282284]. https://doi.org/10.1016/S1470-2045(14)70387-0.
4. Fintelmann FJ, Brinkmann JK, Jeck WR, Troschel FM, Digumarthy SR, Mino-Kenudson M, et al. Lung Cancers Associated With Cystic Airspaces: Natural History, Pathologic Correlation, and Mutational Analysis. *J Thorac Imaging*. 2017;**32**(3):176–88. [PubMed ID: 28338535]. https://doi.org/10.1097/RTI.0000000000000265.
5. Mascalchi M, Attina D, Bertelli E, Falchini M, Vella A, Pegna AL, et al. Lung cancer associated with cystic airspaces. *J Comput Assist Tomogr*. 2015;**39**(1):102–8. [PubMed ID: 25279848]. https://doi.org/10.1097/RCT.0000000000000154.
6. Haider E, Burute N, Harish S, Boylan C. Lung cancer associated with cystic airspaces: Characteristic morphological features on CT in a series of 11 cases. *Clin Imaging*. 2019;**56**:102–7. [PubMed ID: 31026681]. https://doi.org/10.1016/j.clinimag.2019.02.015.
7. Tan Y, Gao J, Wu C, Zhao S, Yu J, Zhu R, et al. CT Characteristics and Pathologic Basis of Solitary Cystic Lung Cancer. *Radiology*. 2019;**291**(2):495–501. [PubMed ID: 30860446]. https://doi.org/10.1148/radiol.2019181598.
8. Sheard S, Moser J, Sayer C, Stefanidis K, Devaraj A, Vlahos I. Lung Cancers Associated with Cystic Airspaces: Underrecognized Features of Early Disease. *Radiographics*. 2018;**38**(3):704–17. [PubMed ID: 29652577]. https://doi.org/10.1148/rg.2018170099.
9. Scholten ET, Horeweg N, de Koning HJ, Vliegenthart R, Oudkerk M, Mali WP, et al. Computed tomographic characteristics of interval and post screen carcinomas in lung cancer screening. *Eur Radiol*. 2015;**25**(1):81–8. [PubMed ID: 25187382]. https://doi.org/10.1007/s00330-014-3394-4.
10. MacMahon H, Naidich DP, Goo JM, Lee KS, Leung ANC, Mayo JR, et al. Guidelines for Management of Incidental Pulmonary Nodules Detected on CT Images: From the Fleischner Society 2017. *Radiology*. 2017;**284**(1):228–43. [PubMed ID: 28240562]. https://doi.org/10.1148/radiol.2017161659.
11. Byrne D, English JC, Atkar-Khattra S, Lam S, Yee J, Myers R, et al. Cystic Primary Lung Cancer: Evolution of Computed Tomography Imaging Morphology Over Time. *J Thorac Imaging*. 2021;**36**(6):373–81. [PubMed ID: 34029281]. https://doi.org/10.1097/RTI.0000000000000594.
12. Landis JR, Koch GG. The measurement of observer agreement for categorical data. *Biometrics*. 1977;**33**(1):159–74. [PubMed ID: 843571].
13. Snoeckx A, Reyntiens P, Carp L, Spinhoven MJ, El Addouli H, Van Hoyweghen A, et al. Diagnostic and clinical features of lung cancer associated with cystic airspaces. *J Thorac Dis*. 2019;**11**(3):987–1004. [PubMed ID: 31019789]. [PubMed Central ID: PMC6462709]. https://doi.org/10.21037/jtd.2019.02.91.
14. Farooqi AO, Cham M, Zhang L, Beasley MB, Austin JH, Miller A, et al. Lung cancer associated with cystic airspaces. *AJR Am J Roentgenol*. 2012;**199**(4):781–6. [PubMed ID: 22997368]. https://doi.org/10.2214/AJR.11.7812.
15. Guo J, Liang C, Sun Y, Zhou N, Liu Y, Chu X. Lung cancer presenting as thin-walled cysts: An analysis of 15 cases and review of literature. *Asia Pac J Clin Oncol*. 2016;**12**(1):e105–12. [PubMed ID: 24354425]. https://doi.org/10.1111/ajco.12126.
16. Mendoza DP, Heeger A, Mino-Kenudson M, Lanuti M, Shepard JO, Sequist LV, et al. Clinicopathologic and Longitudinal Imaging Features of Lung Cancer Associated With Cystic Airspaces: A Systematic Review and Meta-Analysis. *AJR Am J Roentgenol*. 2021;**216**(2):318–29. [PubMed ID: 32755209]. https://doi.org/10.2214/AJR.20.23835.
17. Kunihiro Y, Kobayashi T, Tanaka N, Matsumoto T, Okada M, Kamiya M, et al. High-resolution CT findings of primary lung cancer with cavitation: a comparison between adenocarcinoma and squamous cell carcinoma. *Clin Radiol*. 2016;**71**(11):1126–31. [PubMed ID: 27394062]. https://doi.org/10.1016/j.crad.2016.06.110.
18. Deng H, Zhang J, Zhao S, Zhang J, Jiang H, Chen X, et al. Thin-wall cystic lung cancer: A study of 45 cases. *Oncol Lett*. 2018;**16**(1):755–60. [PubMed ID: 29963142]. [PubMed Central ID: PMC6019975]. https://doi.org/10.3892/ol.2018.8707.
19. Xue X, Wang P, Xue Q, Wang N, Zhang L, Sun J, et al. Comparative study of solitary thin-walled cavity lung cancer with computed tomography and pathological findings. *Lung Cancer*. 2012;**78**(1):45–50. [PubMed ID: 22784387]. https://doi.org/10.1016/j.lungcan.2012.06.004.
20. Nambu A, Miyata K, Ozawa K, Miyazawa M, Taguchi Y, Araki T. Air-containing space in lung adenocarcinoma: high-resolution computed tomography findings. *J Comput Assist Tomogr*. 2002;**26**(6):1026–31. [PubMed ID: 12488755]. https://doi.org/10.1097/00004728-200211000-00030.
21. Koizumi N, Akita S, Sakai K, Oda J, Tsukada H, Usuda H, et al. Classification of air density areas in CT-pathologic correlation of pulmonary adenocarcinoma. *Radiat Med*. 1995;**13**(6):279–84. [PubMed ID: 8850368].
22. Liu Z, Feng H, Zhang Z, Sun H, Liu D. Clinicopathological characteristics of solitary cavitary lung cancer: a case-control study. *J Thorac Dis*. 2020;**12**(6):3148–56. [PubMed ID: 32642236]. [PubMed Central ID: PMC7330766]. https://doi.org/10.21037/jtd-20-426.